

Single-pass transcription by T7 RNA polymerase

LUIZ F.M. PASSALACQUA,^{1,4} ARMINE I. DINGILIAN,¹ and ANDREJ LUPTÁK^{1,2,3}

¹Department of Pharmaceutical Sciences, ²Department of Chemistry, ³Department of Molecular Biology and Biochemistry, University of California, Irvine, California 92697, USA

ABSTRACT

RNA molecules can be conveniently synthesized *in vitro* by the T7 RNA polymerase (T7 RNAP). In some experiments, such as cotranscriptional biochemical analyses, continuous synthesis of RNA is not desired. Here, we propose a method for a single-pass transcription that yields a single transcript per template DNA molecule using the T7 RNAP system. We hypothesized that stalling the polymerase downstream from the promoter region and subsequent cleavage of the promoter by a restriction enzyme (to prevent promoter binding by another polymerase) would allow synchronized production of a single transcript per template. The single-pass transcription was verified in two different scenarios: a short self-cleaving ribozyme and a long mRNA. The results show that a controlled single-pass transcription using T7 RNAP allows precise measurement of cotranscriptional ribozyme activity, and this approach will facilitate the study of other kinetic events.

Keywords: cotranscriptional activity; folding; self-scission

INTRODUCTION

In vitro transcription is used in studies ranging from biochemical analyses of functional RNAs to downstream events (Beckert and Masquida 2011; Wang et al. 2018), for example in mRNA translation, RNA nanotechnology (Grabow and Jaeger 2014; Yesselman et al. 2019), and structural biology (Ahmed and Ficner 2014). RNA molecules can be conveniently synthesized *in vitro*, generating single-stranded transcripts that range from a few nucleotides (nt) to thousands of nt in length (Beckert and Masquida 2011). The most commonly used enzyme for *in vitro* transcription is the T7 RNA polymerase (T7 RNAP), which has been studied extensively over the past 50 years (Borkotoky and Murali 2018; Wang et al. 2018). In contrast to multisubunit RNAPs found in bacteria, Archaea, and eukaryotes, the T7 bacteriophage-derived RNAP is a single subunit (98 kDa) enzyme that does not need any additional factors to initiate and sustain transcription (Borkotoky and Murali 2018; Wang et al. 2018). The enzyme has a high specificity toward the T7 promoter sequence, allowing precise transcription initiation (Milligan et al. 1987; Rong et al. 1998; Imburgio et al. 2000; Beckert and Masquida 2011; Borkotoky and Murali 2018; Wang et al. 2018).

The ability to generate up to milligram quantities of transcripts using the T7 RNAP system has resulted in a multitude of adaptations in molecular biology (Milligan et al. 1987; Milligan and Uhlenbeck 1989; Beckert and Masquida 2011). While the T7 RNAP system has been invaluable for *in vitro* studies of RNA, there are many situations in which large quantities and continuous synthesis of RNA are not desired. Many studies use T7-RNAP-transcribed RNAs that are purified under denaturing conditions, a step that can result in misfolded RNAs (Uhlenbeck 1995), because *in vitro* refolding causes RNA molecules to lose their folding directionality (5' to 3'), likely resulting in the coexistence of different folding states (Pan et al. 1999; Diegelman-Parente and Bevilacqua 2002). Purification conditions that are less harsh, such as nondenaturing chromatography, have been utilized for well-defined transcripts (Lupták et al. 2001; Kieft and Batey 2004; Batey and Kieft 2007; Toor et al. 2008). A different approach to biochemical characterization of RNAs includes cotranscriptional *in vitro* experiments with continuous transcription, but the kinetics of the RNA synthesis over time must be taken into account, leading to increasingly complex models (Long and Uhlenbeck 1994; Mercure et al. 1998). Another alternative for the study of

⁴**Present address:** Laboratory of RNA Biophysics and Cellular Physiology, National Heart, Lung, and Blood Institute—National Institutes of Health, Bethesda, Maryland 20892, USA

Corresponding author: aluptak@uci.edu

Article is online at <http://www.majournal.org/cgi/doi/10.1261/rna.076778.120>.

© 2020 Passalacqua et al. This article is distributed exclusively by the RNA Society for the first 12 months after the full-issue publication date (see <http://majournal.cshlp.org/site/misc/terms.xhtml>). After 12 months, it is available under a Creative Commons License (Attribution-NonCommercial 4.0 International), as described at <http://creativecommons.org/licenses/by-nc/4.0/>.

cotranscriptional events is to terminate the transcription reaction with a dilution into new conditions that prevent any new RNA synthesis, thereby avoiding the need to account for the kinetics of transcription (Passalacqua et al. 2017; Passalacqua and Lupták 2021). This method, however, may not be suitable for experiments that require specific conditions, such as the volume-limited or highly synchronized transcriptions that are used in some coupled transcriptional–translational studies, single-molecule studies, and other biophysical experiments. A simple and effective method that generates precise amounts of RNA and enables temporal control throughout the experiment is thus desirable for cotranscriptional studies using the T7 RNAP system.

Here we present a method for a single-pass transcription that yields a single transcript per template DNA molecule. We hypothesized that stalling the T7 RNAP downstream from the promoter region and subsequent cleavage of the promoter by a restriction enzyme (to prevent promoter rebinding by another T7 RNAP) will generate single transcripts. In this study, two RNA models were utilized for transcription. The first is the HDV-like self-cleaving ribozyme drz-Fpra-2 (Webb and Lupták 2011; Passalacqua et al. 2017), a catalytic RNA molecule that promotes a site-specific self-scission reaction (Jimenez et al. 2015). This model system allows tracking of both the synthesis of the full-length construct and the fidelity and folding of the nascent transcript through the formation of the cleaved product. The second model, a longer construct, is the mRNA of the *Thermus aquaticus* DNA polymerase (Klentaq) (Barnes 1992). We compare the method with transcription inhibition by heparin, a widely used polymerase inhibitor.

RESULTS

T7 RNAP stalling position and strategy for promoter cleavage

The promoter sequence of the T7 RNAP consists of a 23-base pair (bp) region that extends from the position -17 to the position $+6$, where $+1$ is the first nucleotide to be transcribed (Rosa 1979; Imburgio et al. 2000). The consensus sequence found in T7 bacteriophage promoters is 5'-TAATACGACTCACTATAGGGAGA; the first nucleotides to be transcribed are underlined (Imburgio et al. 2000). It can be separated into two domains: an upstream binding region that extends from position -17 to -5 , and a downstream initiation region from -4 to $+6$ (Rosa 1979; Chapman and Burgess 1987; Chapman et al. 1988; Li et al. 1996; Rong et al. 1998; Imburgio et al. 2000). At the initiation region, substitutions are, in general, well-tolerated in the first transcribed nucleotides, with the exception of substitutions at the position $+1$, in which no variation is tolerable, and the position $+2$, where nonconsensus mutations reduce the transcription yield by half

(Imburgio et al. 2000). Thus, for efficient RNA production, the first transcribed nucleotide should remain unchanged; however, optimal results are obtained when the entire binding region and the first six nucleotides (-4 to $+2$) of the T7 consensus initiation sequence are maintained (Imburgio et al. 2000).

The T7 RNAP promoter with GGGAGA sequence at the initiation region can be targeted by four commercially available restriction enzymes that recognize at least 4 bp of the consensus sequence: MlyI, PstI, SfiI, and HinfI (Roberts et al. 2015). We chose HinfI, a type-II restriction endonuclease that recognizes the GANTC sequence, where N is any base, and cleaves between guanine and adenine residues on both strands of the DNA duplex (positions -10 and -11 of the promoter sequence) (Osterman and Coleman 1981; Roberts 1981; Frankel et al. 1985; Roberts et al. 2015). HinfI has previously been used in studies of T7 RNAP promoter recognition and its activity was shown to prevent transcription (Osterman and Coleman 1981). The HinfI enzyme has a monomeric molecular weight of 31 kDa, and like other restriction enzymes, is active in dimer form (Frankel et al. 1985) and depends on Mg^{2+} for catalysis (Pingoud et al. 2005). The molecular architecture of HinfI is not known, but the structural similarity among type-II restriction endonucleases allows estimation of the spatial organization of HinfI around its DNA binding site (Pingoud 2001; Pingoud et al. 2005). In addition, DNase footprinting studies of distinct type-II restriction enzymes have shown that they protect 13–21 bp of the target DNA (Fox 1988).

Biochemical and structural studies of the T7 RNAP showed that the transcription bubble comprises a stretch of 17 nt, with an overall interaction with about 20 nt of the DNA template (Ikeda and Richardson 1986; Chapman et al. 1988; Martin et al. 1988; Sousa 1996; Montesana et al. 2000; Yin and Steitz 2002; Durniak et al. 2008). The RNA polymerase can be stalled by depleting a specific nucleotide from the reaction mixture (Levin et al. 1987; Erie et al. 1992; Sohn et al. 2003), but guanosine cannot be the stalling nucleotide, because the T7 RNAP requires guanosines for efficient transcription initiation (Imburgio et al. 2000). T7 RNAP complexes stalled within the first 8–10 nt of the RNA transcript are less stable because they are in the transcription-initiation conformation, whereas complexes stalled at a later position (during the elongation stage of transcription) are highly processive and therefore more stable, resulting in fewer abortive events (Ling et al. 1989; Montesana et al. 2000; Zhou and Martin 2006). Furthermore, stalling the T7 RNAP away from the promoter region gives the restriction enzyme enough room to cleave the promoter region without sterically clashing with the T7 RNAP elongation complex. For these reasons, we chose to stall the T7 RNAP at position $+27$ by incorporating the first cytosine at this position and initiating transcription using only GTP, ATP, and UTP. Once the T7 RNAP is stalled at the $+27$ position, the restriction enzyme is added to cleave

the polymerase-free promoter and prevent new transcription initiation. Subsequent addition of CTP facilitates the synthesis of the full-length transcript (Fig. 1).

T7 RNAP promoter cleavage by a restriction enzyme and single-pass transcription optimization

To study the cleavage of the T7 promoter region of the transcribed DNA, we measured the kinetics of the cleavage reaction by the HinfI restriction enzyme under various conditions. For these studies, HinfI was used at a concentration of ~65 nM and the DNA template at 100 nM. We first investigated the cleavage reaction in the transcription reaction mixture (reaction buffer+rNTPs) without the T7 RNAP (Fig. 2A). About 40% of the DNA was cleaved after 1 minute, ~85% after 3 min, and no full-length construct was detected after 6 min of reaction. Next, we probed the binding competition between T7 RNAP (100 nM final concentration) and HinfI. To allow the binding of the T7 RNAP to the promoter region, we waited 3 min before adding HinfI to the reaction. We also avoided the addition of rNTPs to ensure that the T7 RNAP does not initiate transcription and move downstream from the promoter region. Surprisingly, the cleavage reaction occurred slightly faster in the presence of T7 RNAP. After 1 min of incubation, about 60% of the DNA was cleaved; after 3 min, ~85% was cleaved; and no full-length DNA was detected after 6 min of digestion (Fig. 2B). The result obtained here is in accordance with previous studies of T7 RNAP promoter showing that HinfI outcompetes the T7 RNAP for the promoter binding and cleavage (Osterman and Coleman 1981). This result also indicates that the endonuclease does not need to be in excess for the cleavage reaction to reach completion.

To pause the T7 RNAP downstream from the promoter region and allow DNA cleavage by HinfI, we performed the same experiment in the presence of GTP, ATP, and

UTP. This stalling experiment demonstrates that the HinfI cleavage is faster than the two previous experiments, with no detectable full-length DNA remaining after 3 min

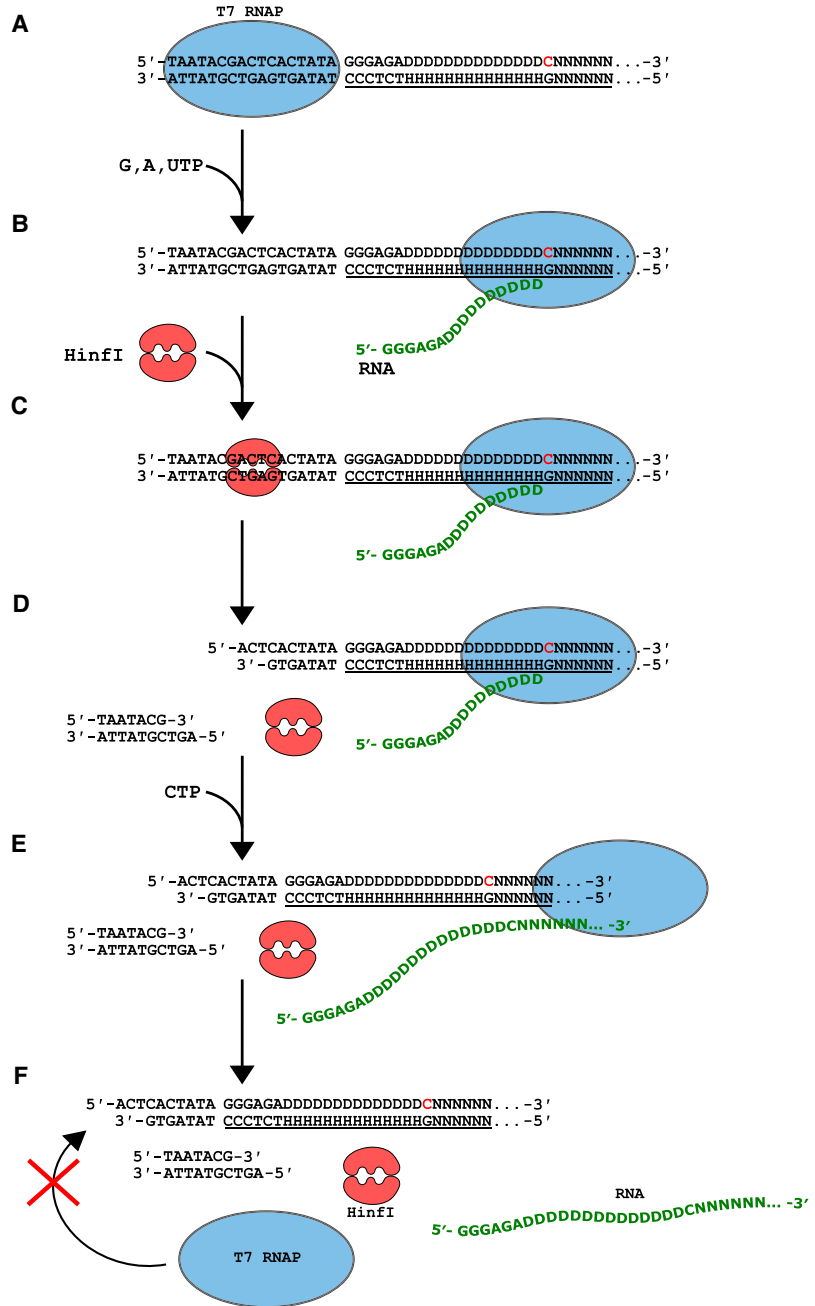


FIGURE 1. Scheme of a single-pass transcription by the T7 RNA polymerase. Transcribed template is underlined, and the first cytosine is shown in red as part of the nontemplate strand. D = A or G or T (not C); H = A or C or T (not G). T7 RNAP (blue oval) binds the promoter of the template DNA (A). Upon the addition of GTP, ATP, and UTP, transcription is initiated, stalling at the first cytosine position (B). Addition of HinfI to the solution while T7 RNAP is stalled downstream from the promoter region allows binding (C) and cleavage of the promoter (D). Subsequent addition of CTP allows the T7 RNAP to continue the synthesis of the transcript (E). Due to the cleaved promoter, the T7 RNAP is unable to start a new transcription reaction (F).

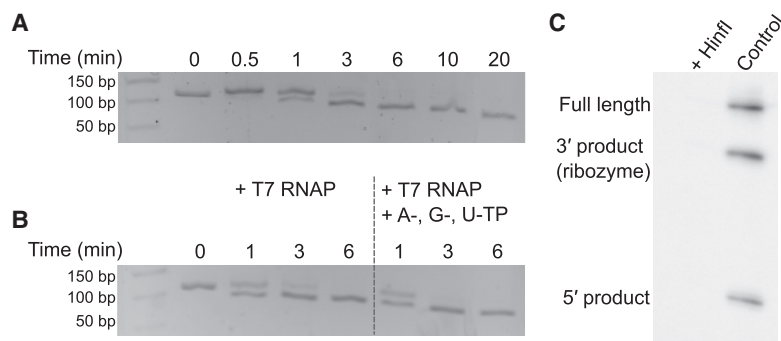


FIGURE 2. Cleavage of the T7 RNAP promoter by Hinfl. (A) Kinetics of the promoter cleavage by Hinfl in a reaction mixture containing NTPs. (B) Kinetics of the promoter cleavage by Hinfl in the presence of T7 RNAP and absence (*left*) or presence of ATP, GTP, and UTP (*right*). (C) Denaturing PAGE analysis of the drz-Fpra-2 ribozyme transcription reaction after Hinfl digestion of the nonstalled T7 RNAP complex (prior to addition of NTPs) compared to the nondigested control reaction.

of reaction (Fig. 2B). The T7 RNAP was clear of the promoter region when Hinfl was added to the reaction, and the results suggest that the action of Hinfl in the promoter region is facilitated by an RNAP that is stalled downstream from the promoter region.

To confirm that the digestion of the promoter by Hinfl is effective at inhibiting the RNA synthesis by the T7 RNAP as previously reported (Osterman and Coleman 1981), we performed a transcription reaction where we incubated the DNA template of the self-cleaving ribozyme drz-Fpra-2 with Hinfl for 10 min before the addition of NTPs to allow transcription to initiate. A control experiment without Hinfl incubation was also performed. As expected, after the addition of NTPs and 10 min of incubation, no product formation was observed in the Hinfl treated experiment, while normal amounts of RNA were detected in the control sample (Fig. 2C).

We also tested the same cleavage reaction by Hinfl with a DNA template containing an antigenomic hepatitis delta virus (aHDV) ribozyme construct (Kuo et al. 1988; Passalacqua et al. 2017) with the first cytosine at position +11—the earliest position to form a stable complex in the elongation phase (Ling et al. 1989; Montesana et al. 2000; Zhou and Martin 2006). The experiment revealed that when the T7 RNAP is stalled at position +11, the cleavage of the promoter by Hinfl is inhibited, by about fivefold, taking more than 6 min to fully cleave the promoter (Supplemental Fig. S1a). This result supports our hypothesis that a downstream stalling site is more suitable for promoter cleavage to avoid a potential steric clash between the two enzymes. To confirm single-pass transcription from the aHDV ribozyme template, we tested the transcription reaction starting from the stalled complex. As expected, before the addition of CTP, the transcripts were stalled and no full-length product observed, whereas after the addition of CTP, full-length product was detected, but further accumu-

lation was observed only in the control experiment lacking Hinfl digestion (Supplemental Fig. S1b). Lastly, we attempted the same experiment using two constructs containing the first cytosines at positions +6 and +7. We expected T7 RNAP complex to be in an abortive initiation phase (Ling et al. 1989; Montesana et al. 2000; Zhou and Martin 2006), and indeed we did not observe any transcription or stalled complex when digested with Hinfl after incubation with T7 RNAP. Taken together, a single-pass transcription can be achieved with transcription complexes stalled at any position in the elongation phase (downstream from position +10), but efficient promoter cleavage by Hinfl

is achieved with T7 RNAP complexes stalled further downstream, where the probability of a steric clash is minimal, such as at position +27.

During the optimization process of the single-pass transcription reaction, we tested different concentrations of Hinfl in the cleavage assay (Supplemental Fig. S2a), and the results showed that the restriction enzyme was active at substoichiometric concentrations. We therefore chose to use Hinfl at a concentration of ~65 nM, lower than the DNA and T7 RNAP concentrations (~100 nM each) in all single-pass transcription experiments. To ensure complete promoter digestion in all experiments, we incubated Hinfl in the reaction mixture for 10 min before addition of the fourth nucleotide. Because previous experiments suggested that the T7 RNAP can form a stable stalled complex in the elongation mode (Zhou and Martin 2006), whereas others suggested that the T7 RNAP can abort the transcript (Koh et al. 2018), we chose not to incubate longer than 10 min before continuing with single-pass transcription.

To test our proposed method for any residual transcription after the initial round of RNA production, we used two different approaches: (i) we added 2 μ M of T7 promoter decoy with CTP to compete for any undigested DNA template and prevent a new round of transcription initiation, and (ii) we added proteinase K enzyme 45 sec after the addition of CTP to promote the digestion of the T7 RNAP after the single round of transcription was completed. In both experiments, the results showed similar behavior to the single-pass transcription, suggesting that no new transcripts were synthesized (Supplemental Fig. S2b). We also observed that the optimal concentration of rNTPs to be used in the reaction is 200 μ M GTP; 100 μ M ATP and UTP; and 50 μ M CTP. Additionally, to avoid a possible accumulation of multiple polymerases and/or transcripts per DNA molecule, we used 1.3-fold excess of DNA template relative to T7 RNAP.

Synthesis of a ribozyme using single-pass transcription

To test the single-pass transcription system utilizing T7 RNAP and *Hin*I, we studied the RNA synthesis and the cotranscriptional self-cleavage reaction of the HDV-like self-cleaving ribozyme drz-Fpra-2 (Passalacqua et al. 2017). A control transcription experiment of drz-Fpra-2 without *Hin*I showed that transcripts and cleaved fractions of the ribozyme accumulate over time due to a continuous synthesis and self-scission of the ribozyme (Fig. 3). We also observed a decrease in transcription rate over time, likely due to the limited amount of rNTPs used in the reaction (200 μ M GTP; 100 μ M ATP and UTP; and 50 μ M CTP) and the resulting scarcity of free rNTPs after a few minutes of reaction. Next, we performed the same experiment but with the addition of the *Hin*I-digestion and showed that the synthesis of RNA proceeds in agreement with a single-pass transcription model and is largely finished 10

sec after the addition of CTP (Fig. 3). Given that the speed of RNA synthesis by the T7 RNAP is around 200–260 nt/sec (Brakmann and Grzeszik 2001), 10 sec is expected to be sufficient time to synthesize the 109-nt-long transcript, even if the reaction includes a lag phase of 1–5 sec, as reported previously (Jia and Patel 1997; Skinner et al. 2004; Tang et al. 2009; Koh et al. 2018). Because this transcript is a ribozyme, the full-length transcript self-cleaves into two shorter products, making it easier to detect continual transcription (Fig. 3). The results confirmed that only a single-pass transcription took place, validating the proposed method.

To confirm that the single-pass methodology does not affect the kinetics of the ribozyme cleavage, we compared the initial rates of cleavage for control and single-pass experiments. The ribozyme self-scission kinetics were analyzed by fitting the first four time points (up to 1-min transcription reaction after the addition of CTP) to a mono-exponential decay function (Eq. 1). The observed rates of self-scission were similar for both the control and the single-pass experiments (Supplemental Fig. S3), supporting our hypothesis that the single-pass would not interfere with the kinetics of the ribozyme reaction. The results obtained here show a lower rate of self-cleavage when compared with a previously reported rate (Passalacqua et al. 2017). This variation is likely due to differences in conditions (buffer, ionic strength, and NTPs concentration) and methodology, as the previously reported experiment was based on a transcription with minimal Mg^{2+} , followed by a 25-fold dilution into a physiological-like buffer (Passalacqua et al. 2017), which is different from the conditions used here.

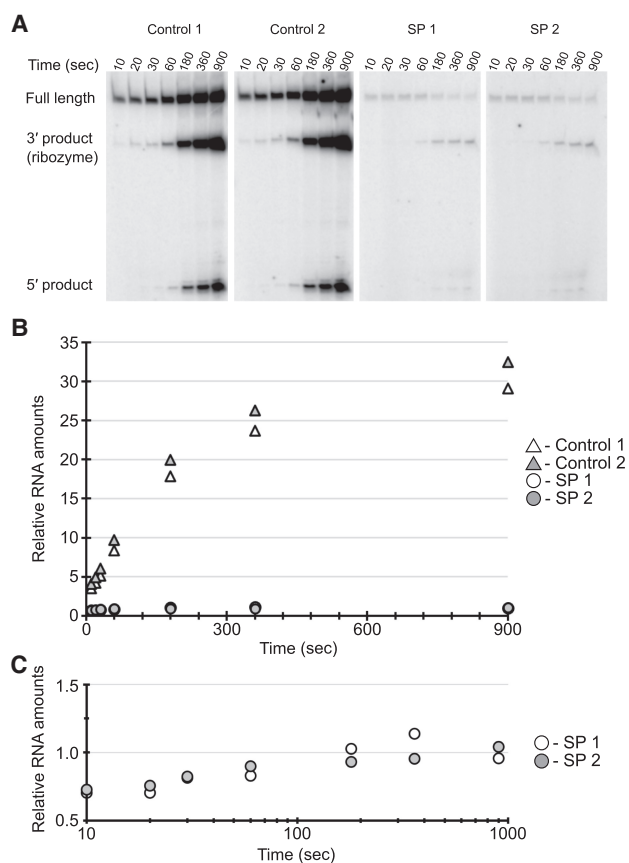


FIGURE 3. Cotranscriptional self-scission of the drz-Fpra-2 ribozyme. (A) Denaturing PAGE analysis of the drz-Fpra-2 ribozyme transcription reaction in the absence (Controls 1 and 2—triangles) and presence of *Hin*I (SP 1 and 2; single-pass transcriptions—circles). (B) Comparison of the relative RNA synthesis over time. (C) Linear-log profile of the RNA synthesis over time for SP1 and SP2. (B,C) Normalized to the average value of SP 1 and 2 at the 900-sec timepoint.

Synthesis of a long transcript using single-pass transcription

We also analyzed the production of an 1831-nt-long transcript, the mRNA of the KlenTaq DNA polymerase, following the same protocol. The *Hin*I-treated experiment showed that most of the RNA was synthesized within 15 sec after the addition of CTP, contrasting with the increasing accumulation of transcripts over time in the control experiment (Fig. 4). As in the ribozyme experiment, we also noticed a decrease in transcription rate over time, likely due to the scarcity of free rNTPs. Because of their size, the majority of the transcripts were stranded near the wells of the PAGE gel. Given that the purpose of this experiment is to verify the synthesis of total RNA, we decided to analyze all the bands near the wells in addition to other visible bands present in the exposed denaturing PAGE gel (Fig. 4). These results support a model of a single-pass transcription of the template. Considering the average speed of the T7 RNAP, about 9 sec are needed for the synthesis of the full transcript, totaling 9–14 sec if we account for a lag phase, confirming that the system

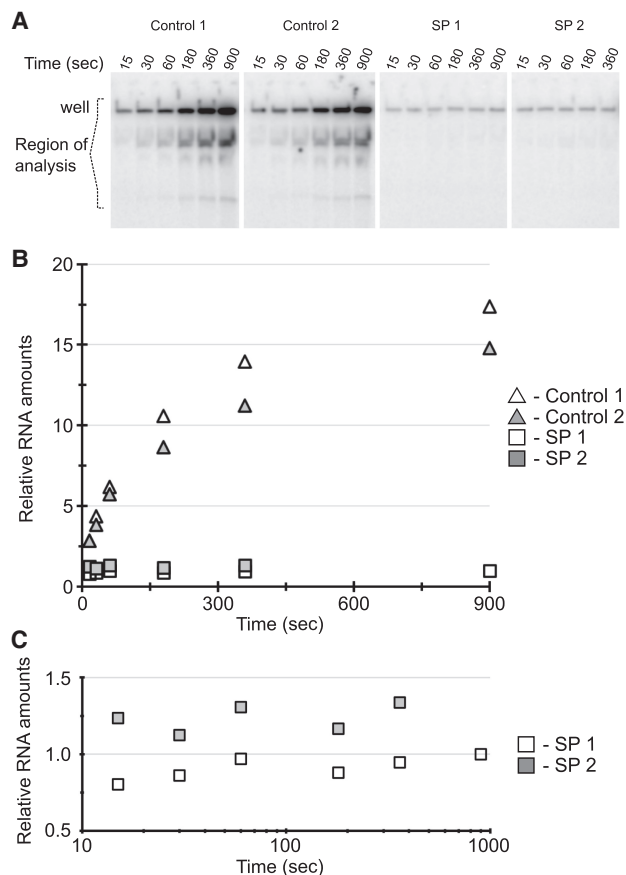


FIGURE 4. Transcription of a long construct. (A) Denaturing PAGE analysis of the *KlenTaq* DNA polymerase gene transcription reaction in the absence (Controls 1 and 2—triangles) and presence of *Hin*I (SP 1 and 2—squares). The last timepoint of SP 2 experiment was removed due to artifact in the PAGE gel. (B) Comparison of the relative RNA synthesis over time. (C) Linear-log profile of the RNA synthesis over time for SP1 and SP2. (B,C) Normalized to the value of SP 1 at the 900-sec timepoint.

is suitable for a controlled synthesis of single RNAs using the T7 RNAP.

Heparin does not fully inhibit T7 RNAP

To compare our method to previously proposed approaches of single-pass RNA synthesis, we tested RNAP inhibition by heparin. Heparin is a competitive inhibitor of RNA polymerases that are widely used to reduce the formation of new initiation complexes, while not affecting transcriptional complexes already in the elongation state (Walter et al. 1967). Previous reports showed that heparin also affects the T7 RNAP elongation complex and that full inhibition is not achieved (Chamberlin and Ring 1973; Sastry and Ross 1997). In early studies of T7 RNAP inhibition by heparin, 20 $\mu\text{g}/\text{mL}$ of heparin was used to inhibit 0.1 μg of T7 RNAP (Chamberlin and Ring 1973), and in a more recent study, 100 $\mu\text{g}/\text{mL}$ was used to inhibit 0.02 μg of T7 RNAP

(Ma et al. 2005). We chose to use this higher concentration of 100 $\mu\text{g}/\text{mL}$ of heparin to test the inhibition of 0.3 μg of T7 RNAP. We compared heparin inhibition of the T7 RNAP to the *Hin*I cleavage using the same conditions and constructs as described above. Despite greatly reducing the activity of the T7 RNAP, we did not observe full inhibition by heparin, and a significant quantity of RNA accumulated over time, relative to the *Hin*I experiment (Supplemental Fig. S4). Thus, the use of heparin is not suitable for single-pass transcription by the T7 RNAP.

DISCUSSION

Our results show that a single-pass transcription is achieved after stalling the T7 RNAP downstream from the promoter region and then rapidly cleaving the promoter region with the restriction enzyme *Hin*I. The single-pass transcription indicated a single read of the DNA template and stopped the accumulation of transcripts within a few seconds, whereas the control experiments showed accumulation of transcripts over time (Figs. 3, 4). Observed initial rates of self-scission for both the control and single-pass experiments were similar, suggesting that the method used in the single-pass transcription does not affect the ribozyme activity (Supplemental Fig. S3). The single-pulse of transcription using the T7-RNAP-*Hin*I system also shows significantly better control of the RNA copy number than a heparin-inhibited reaction (Supplemental Fig. S4). It is important to note that the system proposed here also has disadvantages, particularly if the DNA to be transcribed has another *Hin*I restriction site. In such a case, a single-stranded DNA template with double-stranded promoter region can be used, because a duplex DNA is not required by the T7 RNAP for the elongation phase of transcription (Milligan et al. 1987; Maslak and Martin 1993). An alternative approach would be to use another restriction endonuclease or a nicking endonuclease, such as a type IIS restriction enzyme that would require the addition of a 5' recognition site and would cleave the downstream T7 RNAP promoter region. The choice of a different restriction enzyme and its binding site should be chosen such that the cleavage occurs downstream from the position -12 of the promoter, because the positions -17 to -13 are dispensable for initiation, despite some penalty in yield (Osterman and Coleman 1981; Martin and Coleman 1987; Chapman et al. 1988). Additionally, no 3' overhangs should be created by the restriction enzyme because T7 RNAP can nonspecifically initiate transcription from such sites (Schenborn and Mierendorf 1985; Triana-Alonso et al. 1995).

The simplicity of this method makes it a valuable alternative to purification or dilution of the reaction to halt transcription, simplifying the kinetic studies of cotranscriptional events, such as RNA folding, self-scission, and self-splicing. A continuous transcription reaction is initiated

with all components present at the outset, whereas this approach allows new components (e.g., ligands, cofactors, and modified nucleotides) to be added at a specified point (e.g., before or after the single-pass transcription is performed). The method is not only suitable for studying functional RNAs, such as ribozymes and riboswitches, but can also be adapted to study processes such as cotranscriptional RNA degradation and translation. Biophysical and structural studies of nascent RNAs, including single molecule studies and cryo-EM analyses are also likely to benefit from this method.

MATERIALS AND METHODS

T7 RNAP promoter cleavage by HinfI

Forty microliters reactions were prepared by adding 8 μ L 5 \times reaction buffer (1 \times buffer: 40 mM Tris-HCl, 15 mM Mg(OAc)₂, 50 mM KOAc, 2 mM spermidine, pH 7.5), 4 μ L of 100 mM DTT (10 mM final concentration), and drz-Fpra-2 (Fig. 2A,B) or aHDV (Supplemental Fig. S1a) DNA template (100 nM final concentration). rNTPs were added to a final concentration of 250 μ M each according to the experiment: all four rNTPs for the cleavage analysis without T7 RNAP; GTP, ATP, and UTP for the cleavage analysis for downstream stalled T7 RNAP. No rNTPs were added for the experiment that involved competition for binding at the promoter region. HinfI (NEB) was added at a final concentration of 1% (v/v) (~65 nM). T7 RNAP was used at a final concentration of 100 nM. All reactions were performed at 37°C. Time points were collected and reactions were terminated with an equal volume of stop buffer containing 25 mM EDTA, pH 7.4, with xylene cyanol and bromophenol blue loading dyes. The samples were resolved with 2.5% agarose gel and SYBR Gold staining according to manufacturer's protocol (Invitrogen). The band intensities were analyzed by creating lane profiles for each lane using ImageJ (Schneider et al. 2012).

Transcription reaction of HinfI digested DNA template

Reactions were prepared by mixing 5 \times reaction buffer (1 \times buffer: 40 mM Tris-HCl, 15 mM Mg(OAc)₂, 50 mM KOAc, 2 mM spermidine, pH 7.5), DTT to 10 mM final concentration, T7 RNAP to 100 nM final concentration, and drz-Fpra-2 DNA template to 100 nM final concentration. HinfI was added to ~65 nM final concentration (the control experiment was not incubated with HinfI) and allowed to react for 10 min at 37°C. T7 RNAP was not stalled in this experiment (Fig. 2C). Double-distilled RNase-free water (ddH₂O) was used to complete the reaction volume when needed. After the incubation, rNTPs were added to the reaction to allow transcription to start (200 μ M GTP, CTP, and UTP; 100 μ M ATP). One microliter of [α -³²P]ATP (250 μ Ci/mL) (PerkinElmer) was used to label the transcripts. After 10 min at 37°C, both the HinfI treated reaction and the control reaction were terminated with an equal volume of stop buffer containing 25 mM EDTA, 5 mM Tris pH 7.4, 7 M urea, 0.1% SDS, with xylene cyanol and bromophenol blue loading dyes. The samples were fractionated on a 10% denaturing PAGE gel. The gel was exposed to phosphor-

image screens and analyzed using Typhoon phosphorimager and ImageQuant software (GE Healthcare).

Stoichiometry optimization of DNA, T7 RNAP, rNTPs, and HinfI

Several reactions were performed as described above. Varying concentrations of DNA template (from 50 nM to 1.5 μ M), T7 RNAP (from 50 nM to 2 μ M), HinfI (from 50 nM to 1.5 nM), and rNTPs (from 50 μ M to 500 μ M) were tested to optimize the reaction conditions. We noticed that when the concentration of the T7 RNAP was higher than that of the DNA template, the reaction generated more aborted and background transcripts (data not shown). Our results suggested that a 1:0.75 ratio of DNA:T7 RNAP should be maintained. HinfI proved to be a robust enzyme, and 1% (v/v) (~65 nM) was sufficient to cleave up to 0.5 μ M of DNA in 10 min (data not shown). All reactions were performed at 37°C. Optimal rNTP concentrations for the reaction are as follows: 200 μ M GTP; 100 μ M ATP and UTP; and 50 μ M CTP. Either [α -³²P]ATP or [α -³²P]CTP can be used to track the reaction, but [α -³²P]CTP provides a cleaner PAGE gel because RNAs aborted during transcription initiation are not radiolabeled.

For the HinfI cleavage digestion followed by transcription (Supplemental Fig. S2a), reactions were prepared by mixing 5 \times reaction buffer (1 \times buffer: 40 mM Tris-HCl, 15 mM Mg(OAc)₂, 50 mM KOAc, 2 mM spermidine, pH 7.5), DTT to 10 mM final concentration, T7 RNAP to 1 μ M final concentration, and drz-Fpra-2 DNA template to 1 μ M final concentration. HinfI was added for each sample at the following final concentrations: 1.5 μ M, 1.0 μ M, 0.5 μ M, and 0.25 μ M final concentration (control experiment was not incubated with HinfI). Double-distilled RNase-free water (ddH₂O) was used to complete the reaction volume when needed. NTP final concentrations were 500 μ M GTP, ATP, UTP, and 100 μ M CTP. One microliter of [α -³²P]CTP (250 μ Ci/mL) (PerkinElmer) was used to label the transcripts. T7 RNAP was stalled with the addition of GTP, ATP, and UTP and incubated for 5 min before addition of HinfI enzyme. HinfI digestion was allowed to proceed for 10 min and the transcription reaction was continued with the addition of CTP. After 30 min incubation at 37°C, both the HinfI treated reactions and the control reaction were terminated with an equal volume of stop buffer containing 25 mM EDTA, 5 mM Tris pH 7.4, 7 M urea, 0.1% SDS, with xylene cyanol and bromophenol blue loading dyes.

For the comparison of the single-pass transcription with T7 promoter decoy and proteinase K enzyme digestion (Supplemental Fig. S2b), reactions were prepared by mixing 5 \times reaction buffer (1 \times buffer: 40 mM Tris-HCl, 15 mM Mg(OAc)₂, 50 mM KOAc, 2 mM spermidine, pH 7.5), DTT to 10 mM final concentration, T7 RNAP to 50 nM final concentration, and drz-Fpra-2 DNA template to 200 nM final concentration. HinfI was added for each sample to a final concentration of 400 nM (control experiment was not incubated with HinfI). Double-distilled RNase-free water (ddH₂O) was used to complete the reaction volume when needed. NTP final concentrations were 100 μ M GTP, ATP, CTP, and UTP. A total of 0.25 μ L of [α -³²P]ATP (250 μ Ci/mL) (PerkinElmer) was used to label the transcripts. T7 RNAP was stalled with the addition of GTP, ATP, and UTP and incubated for 5 min before addition of HinfI enzyme. HinfI digestion proceeded for 10 min and the transcription reaction was continued with the addition

of CTP. For the T7 promoter decoy experiment, double-stranded T7 promoter decoy was added to the reaction (final concentration of 2 μ M) with CTP to outcompete any undigested DNA template. For the proteinase K (NEB; 1 unit/50 μ L reaction) experiment, proteolysis of the polymerase was initiated 45 sec after CTP addition. All reactions were performed at 37°C. Time points were collected and the reactions were terminated with an equal volume of stop buffer containing 25 mM EDTA, 5 mM Tris pH 7.4, 7 M urea, 0.1% SDS, with xylene cyanol and bromophenol blue loading dyes. Samples were fractionated on a 10% denaturing PAGE gel. The gel was exposed to phosphorimage screens and analyzed using Typhoon phosphorimager and ImageQuant software (GE Healthcare).

In vitro cotranscriptional analysis

Reactions were prepared by mixing 5 \times reaction buffer (1 \times buffer: 40 mM Tris-HCl, 15 mM Mg(OAc)₂, 50 mM KOAc, 2 mM spermidine, pH 7.5), DTT to 10 mM final concentration, and DNA template (100 nM final concentration for the drz-Fpra-2 and aHDV ribozymes, and 50 nM for the Klentaq DNA polymerase). For the ribozyme experiments, because the self-cleavage reaction requires Mg²⁺ for catalysis (Das and Piccirilli 2005; Chen et al. 2010; Golden 2011; Thaplyal et al. 2015), an additional 2.5 mM MgCl₂ was added to allow self-scission to proceed efficiently. rNTPs were added according to the optimized conditions (200 μ M GTP; 100 μ M ATP and UTP; and 50 μ M CTP). 2 μ L of [α -³²P]CTP (drz-Fpra-2 and Klentaq experiments) or 1 μ L of [α -³²P]ATP (aHDV experiment) (250 μ Ci/mL) (PerkinElmer) was used to label the transcripts. T7 RNAP was added to a final concentration of 75 nM for the ribozyme experiments and 37.5 nM for the Klentaq DNA polymerase experiment. Hinfl was maintained at the optimal final concentration of 1% (v/v) (~65 nM) and was added to the reaction 3 min after the addition of the T7 RNAP. For the heparin experiment, heparin sulfate was used at 100 μ g/mL final concentration, and the reaction followed the same steps as described above. Double-distilled RNase-free water (ddH₂O) was used to complete the reaction volume when needed. CTP addition was used to define t_0 and occurred after a 10-min incubation with Hinfl. All reactions were performed at 37°C. Time points were collected and the reaction was terminated with an equal volume of stop buffer containing 25 mM EDTA, 5 mM Tris pH 7.4, 7 M urea, 0.1% SDS, with xylene cyanol and bromophenol blue loading dyes. Samples were resolved on either a 12% (ribozymes) or a 6% (Klentaq mRNA) denaturing PAGE gel. The gel was exposed to phosphorimage screens and analyzed using Typhoon phosphorimager and ImageQuant software (GE Healthcare). Band intensities were analyzed by creating lane profiles for each lane using ImageJ (Schneider et al. 2012) and exporting the data to Microsoft Excel. Drz-Fpra-2 self-cleavage data were fit to a mono-exponential decay function (Equation 1) for both control and single-pass experiments.

$$\text{Fraction intact} = A \times e^{-kt} + C, \quad (1)$$

where t is time, A represents the relative fractions of the ribozyme population cleaving with a rate constant k , and C represents the ribozyme population that remains uncleaved. The model was fit to the data using a linear least-squares analysis and the Solver module of Microsoft Excel.

SUPPLEMENTAL MATERIAL

Supplemental material is available for this article.

ACKNOWLEDGMENTS

We thank all members of the Lupták laboratory for helpful discussions. This work was supported by Science Without Borders Program—CAPES Foundation, Ministry of Education of Brazil—Process 99999.013571/2013-03 (L.F.M.P.), Miguel Velez Scholarship—UCI (L.F.M.P.), Graduate Dean's Dissertation Fellowship—UCI (L.F.M.P.), and National Science Foundation/Chemical, Bioengineering, Environmental, and Transport Systems (NSF CBET) 1804220 (A.L.).

Author contributions: L.F.M.P. and A.L. designed the study; L.F.M.P. and A.L.D. performed the experiments; all authors analyzed the data; and L.F.M.P. and A.L. wrote the manuscript.

Received June 12, 2020; accepted September 4, 2020.

REFERENCES

- Ahmed YL, Ficner R. 2014. RNA synthesis and purification for structural studies. *RNA Biol* **11**: 427–432. doi:10.4161/rna.28076
- Barnes WM. 1992. The fidelity of Taq polymerase catalyzing PCR is improved by an N-terminal deletion. *Gene* **112**: 29–35. doi:10.1016/0378-1119(92)90299-5
- Batey RT, Kieft JS. 2007. Improved native affinity purification of RNA. *RNA* **13**: 1384–1389. doi:10.1261/rna.528007
- Beckert B, Masquida B. 2011. Synthesis of RNA by in vitro transcription. *Methods Mol Biol* **703**: 29–41. doi:10.1007/978-1-59745-248-9_3
- Borkotoky S, Murali A. 2018. The highly efficient T7 RNA polymerase: a wonder macromolecule in biological realm. *Int J Biol Macromol* **118**: 49–56. doi:10.1016/j.ijbiomac.2018.05.198
- Brakmann S, Grzeszik S. 2001. An error-prone T7 RNA polymerase mutant generated by directed evolution. *Chembiochem* **2**: 212–219. doi:10.1002/1439-7633(20010302)2:3<&212::AID-CBIC212>3.0.CO;2-R
- Chamberlin M, Ring J. 1973. Characterization of T7-specific ribonucleic acid polymerase. II. Inhibitors of the enzyme and their application to the study of the enzymatic reaction. *J Biol Chem* **248**: 2245–2250.
- Chapman KA, Burgess RR. 1987. Construction of bacteriophage T7 late promoters with point mutations and characterization by in vitro transcription properties. *Nucleic Acids Res* **15**: 5413–5432. doi:10.1093/nar/15.13.5413
- Chapman KA, Gunderson SI, Anello M, Wells RD, Burgess RR. 1988. Bacteriophage T7 late promoters with point mutations: quantitative footprinting and in vivo expression. *Nucleic Acids Res* **16**: 4511–4524. doi:10.1093/nar/16.10.4511
- Chen JH, Yajima R, Chadalavada DM, Chase E, Bevilacqua PC, Golden BL. 2010. A 1.9 Å crystal structure of the HDV ribozyme precleavage suggests both Lewis acid and general acid mechanisms contribute to phosphodiester cleavage. *Biochemistry* **49**: 6508–6518. doi:10.1021/bi100670p
- Das SR, Piccirilli JA. 2005. General acid catalysis by the hepatitis delta virus ribozyme. *Nat Chem Biol* **1**: 45–52. doi:10.1038/nchembio703
- Diegelman-Parente A, Bevilacqua PC. 2002. A mechanistic framework for co-transcriptional folding of the HDV genomic ribozyme in the presence of downstream sequence. *J Mol Biol* **324**: 1–16. doi:10.1016/S0022-2836(02)01027-6

- Durniak KJ, Bailey S, Steitz TA. 2008. The structure of a transcribing T7 RNA polymerase in transition from initiation to elongation. *Science* **322**: 553–557. doi:10.1126/science.1163433
- Erie DA, Yager TD, Von Hippel PH. 1992. The single-nucleotide transcription: a biophysical and biochemical perspective. *Annu Rev Biochem* **21**: 379–415.
- Fox KR. 1988. DNAase I footprinting of restriction enzymes. *Biochem Biophys Res Commun* **155**: 779–785. doi:10.1016/S0006-291X(88)80563-1
- Frankel AD, Ackers GK, Smith HO. 1985. Measurement of DNA-protein equilibria using gel chromatography: application to the HinfI restriction endonuclease. *Biochemistry* **24**: 3049–3054. doi:10.1021/bi00333a037
- Golden BL. 2011. Two distinct catalytic strategies in the hepatitis delta virus ribozyme cleavage reaction. *Biochemistry* **50**: 9424–9433. doi:10.1021/bi201157t
- Grabow WW, Jaeger L. 2014. RNA self-assembly and RNA nanotechnology. *Acc Chem Res* **47**: 1871–1880. doi:10.1021/ar500076k
- Ikeda RA, Richardson CC. 1986. Interactions of the RNA polymerase of bacteriophage T7 with its promoter during binding and initiation of transcription. *Proc Natl Acad Sci* **83**: 3614–3618. doi:10.1073/pnas.83.11.3614
- Imburgio D, Rong M, Ma K, McAllister WT. 2000. Studies of promoter recognition and start site selection by T7 RNA polymerase using a comprehensive collection of promoter variants. *Biochemistry* **39**: 10419–10430. doi:10.1021/bi000365w
- Jia Y, Patel SS. 1997. Kinetic mechanism of transcription initiation by bacteriophage T7 RNA polymerase. *Biochemistry* **36**: 4223–4232. doi:10.1021/bi9630467
- Jimenez RM, Polanco JA, Lupták A. 2015. Chemistry and biology of self-cleaving ribozymes. *Trends Biochem Sci* **40**: 648–661. doi:10.1016/j.tibs.2015.09.001
- Kieft JS, Batey RT. 2004. A general method for rapid and nondenaturing purification of RNAs. *RNA* **10**: 988–995. doi:10.1261/rna.7040604
- Koh HR, Roy R, Sorokina M, Tang GQ, Nandakumar D, Patel SS, Ha T. 2018. Correlating transcription initiation and conformational changes by a single-subunit RNA polymerase with near base-pair resolution. *Mol Cell* **70**: 695–706. doi:10.1016/j.molcel.2018.04.018
- Kuo MY, Sharmeen L, Dinter-Gottlieb G, Taylor J. 1988. Characterization of self-cleaving RNA sequences on the genome and antigenome of human hepatitis delta virus. *J Virol* **62**: 4439–4444.
- Levin JR, Krummel B, Chamberlin MJ. 1987. Isolation and properties of transcribing ternary complexes of *Escherichia coli* RNA polymerase positioned at a single template base. *J Mol Biol* **196**: 85–100. doi:10.1016/0022-2836(87)90512-2
- Li T, Ho HH, Maslak M, Schick C, Martin CT. 1996. Major groove recognition elements in the middle of the T7 RNA polymerase promoter. *Biochemistry* **35**: 3722–3727. doi:10.1021/bi9524373
- Ling ML, Risman SS, Klement JF, McGraw N, McAllister WT. 1989. Abortive initiation by bacteriophage T3 and T7 RNA polymerases under conditions of limiting substrate. *Nucleic Acids Res* **17**: 1605–1618. doi:10.1093/nar/17.4.1605
- Long DM, Uhlenbeck OC. 1994. Kinetic characterization of intramolecular and intermolecular hammerhead RNAs with stem II deletions. *Proc Natl Acad Sci* **91**: 6977–6981. doi:10.1073/pnas.91.15.6977
- Lupták A, Ferré-D'Amaré AR, Zhou K, Zilm KW, Doudna JA. 2001. Direct pKa measurement of the active-site cytosine in a genomic hepatitis delta virus ribozyme. *J Am Chem Soc* **123**: 8447–8452. doi:10.1021/ja016091x
- Ma K, Temiakov D, Anikin M, McAllister WT. 2005. Probing conformational changes in T7 RNA polymerase during initiation and termination by using engineered disulfide linkages. *Proc Natl Acad Sci* **102**: 17612–17617. doi:10.1073/pnas.0508865102
- Martin CT, Coleman JE. 1987. Kinetic analysis of T7 RNA polymerase-promoter interactions with small synthetic promoters. *Biochemistry* **26**: 2690–2696. doi:10.1021/bi00384a006
- Martin CT, Muller DK, Coleman JE. 1988. Processivity in early stages of transcription by T7 RNA polymerase. *Biochemistry* **27**: 3966–3974. doi:10.1021/bi00411a012
- Maslak M, Martin CT. 1993. Kinetic analysis of T7 RNA polymerase transcription initiation from promoters containing single-stranded regions. *Biochemistry* **32**: 4281–4285. doi:10.1021/bi00067a017
- Mentesana PE, Chin-Bow ST, Sousa R, McAllister WT. 2000. Characterization of halted T7 RNA polymerase elongation complexes reveals multiple factors that contribute to stability. *J Mol Biol* **302**: 1049–1062. doi:10.1006/jmbi.2000.4114
- Mercurio S, Lafontaine D, Ananvoranich S, Perreault JP. 1998. Kinetic analysis of δ ribozyme cleavage. *Biochemistry* **37**: 16975–16982. doi:10.1021/bi9809775
- Milligan JF, Uhlenbeck OC. 1989. Synthesis of small RNAs using T7 RNA polymerase. *Methods Enzymol* **180**: 51–62. doi:10.1016/0076-6879(89)80091-6
- Milligan JF, Groebe DR, Witherell GW, Uhlenbeck OC. 1987. Oligoribonucleotide synthesis using T7 RNA polymerase and synthetic DNA templates. *Nucleic Acids Res* **15**: 8783–8798. doi:10.1093/nar/15.21.8783
- Osterman HL, Coleman JE. 1981. T7 Ribonucleic acid polymerase-promoter interactions. *Biochemistry* **20**: 4884–4892. doi:10.1021/bi00520a013
- Pan T, Artsimovitch I, Fang XW, Landick R, Sosnick TR. 1999. Folding of a large ribozyme during transcription and the effect of the elongation factor NusA. *Proc Natl Acad Sci* **96**: 9545–9550. doi:10.1073/pnas.96.17.9545
- Passalacqua LFM, Lupták A. 2021. Co-transcriptional analysis of self-cleaving ribozymes and their ligand dependence. In *Ribozymes: methods and protocols* (ed. Scarborough RJ, Gagnon A), pp. 13–24. Springer US, New York.
- Passalacqua LFM, Jimenez RM, Fong JY, Lupták A. 2017. Allosteric modulation of the *Faecalibacterium prausnitzii* hepatitis delta virus-like ribozyme by glucosamine 6-phosphate: the substrate of the adjacent gene product. *Biochemistry* **56**: 6006–6014. doi:10.1021/acs.biochem.7b00879
- Pingoud A. 2001. Structure and function of type II restriction endonucleases. *Nucleic Acids Res* **29**: 3705–3727. doi:10.1093/nar/29.18.3705
- Pingoud A, Fuxreiter M, Pingoud V, Wende W. 2005. Type II restriction endonucleases: structure and mechanism. *Cell Mol Life Sci* **62**: 685–707. doi:10.1007/s00018-004-4513-1
- Roberts JR. 1981. Restriction and modification enzymes and their recognition sequences. *Nucleic Acids Res* **9**: 213. doi:10.1093/nar/9.1.213-c
- Roberts RJ, Vincze T, Posfai J, Macelis D. 2015. REBASE—a database for DNA restriction and modification: enzymes, genes and genomes. *Nucleic Acids Res* **43**: D298–D299. doi:10.1093/nar/gku1046
- Rong M, Biao H, McAllister WT, Durbin RK. 1998. Promoter specificity determinants of T7 RNA polymerase. *Proc Natl Acad Sci* **95**: 515–519. doi:10.1073/pnas.95.2.515
- Rosa MD. 1979. Four T7 RNA polymerase promoters contain an identical 23 bp sequence. *Cell* **16**: 815–825. doi:10.1016/0092-8674(79)90097-7
- Sastry SS, Ross BM. 1997. Nuclease activity of T7 RNA polymerase and the heterogeneity of transcription elongation complexes. *J Biol Chem* **272**: 8644–8652. doi:10.1074/jbc.272.13.8644
- Schenborn ET, Mierendorf RC Jr. 1985. A novel transcription property of SP6 and T7 RNA polymerases: dependence on template

- structure. *Nucleic Acids Res* **13**: 6223–6236. doi:10.1093/nar/13.17.6223
- Schneider CA, Rasband WS, Eliceiri KW. 2012. NIH Image to ImageJ: 25 years of image analysis. *Nat Methods* **9**: 671–675. doi:10.1038/nmeth.2089
- Skinner GM, Baumann CG, Quinn DM, Molloy JE, Hoggett JG. 2004. Promoter binding, initiation, and elongation by bacteriophage T7 RNA polymerase: a single-molecule view of the transcription cycle. *J Biol Chem* **279**: 3239–3244. doi:10.1074/jbc.M310471200
- Sohn Y, Shen H, Kang C. 2003. Stepwise walking and cross-linking of RNA with elongating T7 RNA polymerase. *Methods Enzymol* **371**: 170–179. doi:10.1016/S0076-6879(03)71012-X
- Sousa R. 1996. Structural and mechanistic relationships between nucleic acid polymerases. *Trends Biochem Sci* **21**: 186–190. doi:10.1016/S0968-0004(96)10023-2
- Tang GQ, Roy R, Bandwar RP, Ha T, Patel SS. 2009. Real-time observation of the transition from transcription initiation to elongation of the RNA polymerase. *Proc Natl Acad Sci* **106**: 22175–22180. doi:10.1073/pnas.0906979106
- Thaplyal P, Ganguly A, Hammes-Schiffer S, Bevilacqua PC. 2015. Inverse thio effects in the hepatitis delta virus ribozyme reveal that the reaction pathway is controlled by metal ion charge density. *Biochemistry* **54**: 2160–2175. doi:10.1021/acs.biochem.5b00190
- Toor N, Keating KS, Taylor SD, Pyle AM. 2008. Crystal structure of a self-spliced group II intron. *Science* **320**: 77–82. doi:10.1126/science.1153803
- Triana-Alonso FJ, Dabrowski M, Wadzack J, Nierhaus KH. 1995. Self-coded 3'-extension of run-off transcripts produces aberrant products during in vitro transcription with T7 RNA polymerase. *J Biol Chem* **270**: 6298–6307. doi:10.1074/jbc.270.11.6298
- Uhlenbeck OC. 1995. Keeping RNA happy. *RNA* **1**: 4–6.
- Walter G, Zillig W, Palm P, Fuchs E. 1967. Initiation of DNA-dependent RNA synthesis and the effect of heparin on RNA polymerase. *Eur J Biochem* **3**: 194–201. doi:10.1111/j.1432-1033.1967.tb19515.x
- Wang W, Li Y, Wang Y, Shi C, Li C, Li Q, Linhardt RJ. 2018. Bacteriophage T7 transcription system: an enabling tool in synthetic biology. *Biotechnol Adv* **36**: 2129–2137. doi:10.1016/j.biotechadv.2018.10.001
- Webb CHT, Lupták A. 2011. HDV-like self-cleaving ribozymes. *RNA Biol* **8**: 719–727. doi:10.4161/rna.8.5.16226
- Yesselman JD, Eiler D, Carlson ED, Gotrik MR, d'Aquino AE, Ooms AN, Kladwang W, Carlson PD, Shi X, Costantino DA, et al. 2019. Computational design of three-dimensional RNA structure and function. *Nat Nanotechnol* **14**: 866–873. doi:10.1038/s41565-019-0517-8
- Yin YW, Steitz TA. 2002. Structural basis for the transition from initiation to elongation transcription in T7 RNA polymerase. *Science* **298**: 1387–1395. doi:10.1126/science.1077464
- Zhou Y, Martin CT. 2006. Observed instability of T7 RNA polymerase elongation complexes can be dominated by collision-induced "bumping". *J Biol Chem* **281**: 24441–24448. doi:10.1074/jbc.M604369200